Orientation dependence of the polarizability of an individual WS_2 nanotube by resonant Raman spectroscopy

P. M. Rafailov,[1,*] C. Thomsen,[1] K. Gartsman,[2] I. Kaplan-Ashiri,[2] and R. Tenne[2]
[1]*Institut für Festkörperphysik, Technische Universität Berlin, Hardenbergstrasse 36, 10623 Berlin, Germany*
[2]*Weizmann Institute of Science, Rehovot, Israel*
(Received 26 September 2005; published 23 November 2005)

We obtained a Raman signal from an individual WS_2 nanotube mounted on an atomic force microscopy cantilever tip. We discuss the implications for simultaneous investigations of the mechanical properties of WS_2 nanotubes by combining different experimental methods. From the orientation dependence of this nanotube's resonant Raman intensity, we estimate the ratio of the perpendicular to parallel polarizabilities $\alpha_{XX}/\alpha_{ZZ} \approx 0.16$. We compare the WS_2 nanotube with single-walled carbon nanotubes and expect a similarly strong depolarization effect for multiwalled carbon nanotubes.

DOI: 10.1103/PhysRevB.72.205436 PACS number(s): 78.30.Hv, 63.22.+m, 78.67.Ch

I. INTRODUCTION

Raman spectroscopy is a simple and yet powerful technique for combined investigation of the structural and electronic properties of nanosized objects. The importance of such simultaneous studies has been convincingly demonstrated for nanotubes which are highly perspective for both nanomechanical and nanoelectronic applications. So far, mainly carbon nanotubes have been investigated, but nanotubes of other materials, e.g., WS_2 or BN, increasingly attract research interest. Especially WS_2 nanotubes are appropriate as solid lubricants and antishock materials as well as for tips in atomic force microscopy[1] (AFM). The variety of nanotube chiralities and diameters and their one dimensionality make it highly desirable to study individual specimens. Isolated nanotubes are prepared either by dispersing them onto a substrate or by wrapping them in organic matrices in solution. Recently, individual WS_2 multiwalled nanotubes were attached to a cantilever tip of an AFM. This is a very appealing approach for spectroscopic purposes, because the nanotube hangs in free space with a well-defined orientation. Simultaneous mechanical and optical experiments on such a nanotube become possible provided a Raman signal can be obtained from an object with one dimension smaller than the wavelength of light.

Together with the one-dimensional electronic density of states and the quantum confinement, the antenna effect is thus one of the most remarkable manifestations of quasi-one-dimensional systems. Nanotubes provide an almost ideal opportunity for studying the anisotropic polarizability in one-dimensional systems, the so-called antenna effect was predicted for single-walled carbon nanotubes[2,3] (SWNTs). Ajiki and Ando showed that a strong depolarization occurs for radiation polarized perpendicular to the nanotube axis, whereas parallel polarized radiation remains unscreened. An important conclusion for any optical applications of nanotubes was that optical transitions occur only for polarization parallel to the nanotube axis, which was confirmed by a number of optical experiments[4–10] in SWNT.

As a consequence of the screened optical transitions, the resonance Raman intensity of SWNTs strongly varies as a function of the nanotube orientation.[5–10] The antenna effect can be applied to determine the orientation of nanotubes, e.g., when they are embedded in polymers. Krupke *et al.*[11] took advantage of this effect facilitating the separation of semiconducting and metallic SWNTs. In bundles, the influence of the antenna effect was predicted to be weakened by the tube interaction.[12] The antenna effect is thus a measure of the strength of the nanotube interactions. Interestingly, polarized Raman measurements on multiwalled carbon nanotubes (MWNTs) revealed only a small antenna effect.[13,14] On the other hand, the antenna effect was detected in MWNTs by both a depolarization and a multiple-wavelength matching effect known from conventional radiophysics.[15]

In this paper, we report the first Raman measurement on an individual multiwalled WS_2 nanotube mounted in a well-defined orientation at the tip of an AFM. We establish a strong antenna effect comparable to the one in SWNTs, but much larger than in MWNTs. We give a quantitative estimate of the polarizability tensor components of the WS_2 nanotube and compare them to carbon nanotubes. We discuss the feasibility of simultaneous mechanical and optical experiments on individual WS_2 nanotubes.

II. EXPERIMENTAL

Individual WS_2 nanotubes, 2–3 μm long and with 15–25 nm outer diameters, were mounted on cone-shaped AFM cantilevers in the chamber of ESEM XL 30 FEG(FEI) using micromanipulation techniques. The nanotubes were glued to the silicon cantilever by exposing the contact point of the tube to the electron beam, producing amorphous carbon from hydrocarbons in the vacuum chamber. Scanning electron microscopy (SEM) images show that the nanotube is attached to the cone tip and oriented along the cone axis (Fig. 1). The Raman measurements were performed on a Dilor Labram spectrometer, the HeNe-laser $\lambda_{exc}=632.8$ nm (1.96 eV) focused to ≈ 1 μm spot size.

In order to obtain a Raman signal from the individual nanotube, we focused on the cantilever and approached the tip in ≈ 1 μm steps. The WS_2 nanotube signal was maximized just beyond the cantilever tip; note the increasing WS_2

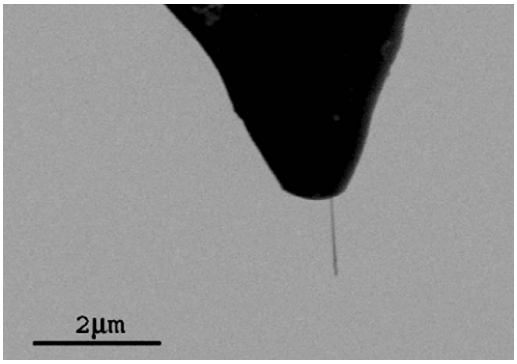

FIG. 1. SEM image of the WS_2 nanotube at the tip of an AFM cantilever. The tube extends downwards.

signal in Fig. 2 (left inset). The Si mode at 520 cm^{-1} was used for calibration. The strongest peaks of WS_2 we identified at 417 and 351 cm^{-1}. They correspond to the A_{1g} and E_{2g} modes, respectively, of the bulk material, and of various WS_2 nanoparticles.[16] For the remainder of this paper, we stay with this notation.

Taking advantage of an oriented specimen, which is rare in nanotube research,[7,8,10,17] we investigated the polarization behavior of the two WS_2 nanotube modes. In Fig. 2, we present *ZZ*, *XZ*, *ZX*, and *XX* spectra (*Z*-nanotube axis). Both the A_{1g} and E_{2g} WS_2 nanotube modes turn out to have the same polarization behavior with a strong signal in *ZZ* geometry only and almost none for *X*-polarized incident or scattered light. This is in striking contradiction to the selection rules for both A_{1g} and E_{2g} symmetries in hexagonal structures.

III. RESULTS AND DISCUSSION

Optical absorption measurements for WS_2 nanotubes are fairly similar to those of the bulk, and Raman spectra of bulk

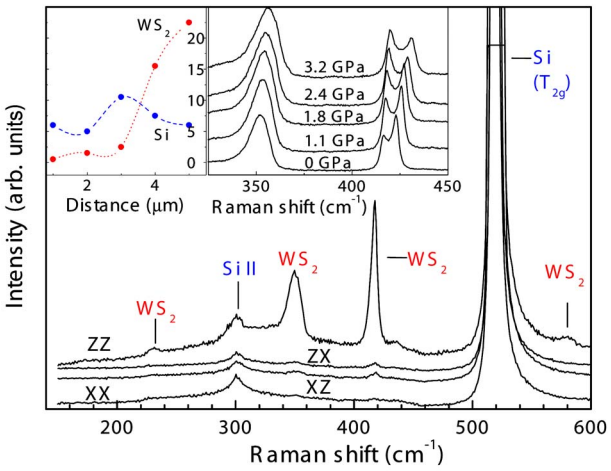

FIG. 2. (Color online) Polarized Raman spectra of a WS_2 nanotube. Note that in addition to the two strong lines described in the text, two other WS_2 nanotube features at 230 and 581 cm^{-1} show up in the *ZZ* spectrum (red). First-order and second-order features of the Si AFM tip are indicated (blue). Inset left: Intensities of spatially resolved measurements performed to locate the WS_2 nanotube. Right: Raman spectra of agglomerated WS_2 nanotubes under hydrostatic pressure.

2H-WS_2, nanoparticles and WS_2 nanotubes look identical down to the smallest details.[16] It is, therefore, safe to approximate the optical and vibrational properties of WS_2 nanotubes by those of bulk WS_2, in analogy to SWNT, MWNT, and graphite.[18] Bulk 2H-WS_2 has a direct gap of 2.05 eV and an exciton energy of 1.95 eV.[16] Hence our excitation (1.96 eV) is in resonance with both the band gap and the *A* exciton. The apparent contradiction between the observed and predicted phonon symmetries may thus be understood by a Raman resonance, which due to the antenna effect should be strongly orientation dependent.[10] The phonon scattering intensity is obtained[19] from the derivative of the polarizability $\hat{\alpha}$ with respect to the normal coordinate q of that mode. In a Lorentz oscillator model with $\hat{\alpha}=\Sigma_j[(e^2\hat{F}_j)/[m(\omega^2-\omega_{0j}^2-i\omega\gamma)]]$

$$\frac{d\hat{\alpha}}{dq}=\sum_j\left[\frac{2\omega_{0j}e^2\hat{F}_j}{m(\omega^2-\omega_{0j}^2-i\omega\gamma)^2}\frac{d\omega_{0j}}{dq}+\frac{e^2}{m(\omega^2-\omega_{0j}^2-i\omega\gamma)}\frac{d\hat{F}_j}{dq}\right], \quad (1)$$

with e and m being the electronic charge and mass, ω as the frequency of the incident radiation, ω_{0j} and $\hat{F}_j$ being the frequency and oscillator-strength tensor, respectively, of the jth electronic transition, and γ as a damping constant.

Near an electronic transition $\omega\approx\omega_{0j}$ and both terms in Eq. (1) are resonantly enhanced. However, the first term dominates through its quadratically vanishing denominator. The Raman tensors of all modes in resonance thus have the same orientation as $\hat{F}_j$, i.e., of the polarizability $\hat{\alpha}$ itself. Note that in particular for smaller-diameter nanotubes $\hat{\alpha}$ and consequently the Raman signal in resonance should be strongly anisotropic. Away from resonance nonresonant Raman scattering dominates with differently oriented Raman tensors.

The observation of the antenna effect is an additional confirmation that the Raman signal was obtained from the individual WS_2 nanotube on the AFM tip. Significantly, this opens the way to simultaneous *in situ* measurements of mechanical properties and Raman spectra. Indeed, buckling[20] and tensile[21] load tests have been recently performed on individual WS_2 nanotubes mounted on an AFM tip. Raman shifts in the vibrational frequencies can be correlated to the elastic response of WS_2 nanotubes. We consider this highly important for many future applications of WS_2 nanotubes such as solid lubricants and antishock materials and tips for AFM studies.

In Fig. 2 (right inset), we show a series of Raman spectra measured under hydrostatic pressure on agglomerated WS_2 nanotubes. We find that the main two Raman modes shift linearly with normalized pressure coefficients $\omega_0^{-1}d\omega/dp\approx 4.5$ TPa^{-1}. Taking a Young modulus[20] of 171 GPa and using the continuum model previously developed for carbon nanotubes,[22] we find axial and circumferential strains of $\varepsilon_{ZZ}=-0.0046p$ and $\varepsilon_{\Theta\Theta}=-0.0087p$. The corresponding linear moduli are $B_Z=220$ GPa and $B_\Theta=115$ GPa showing WS_2 nanotubes to be much more compressible than carbon nanotubes, where these values are approximately one

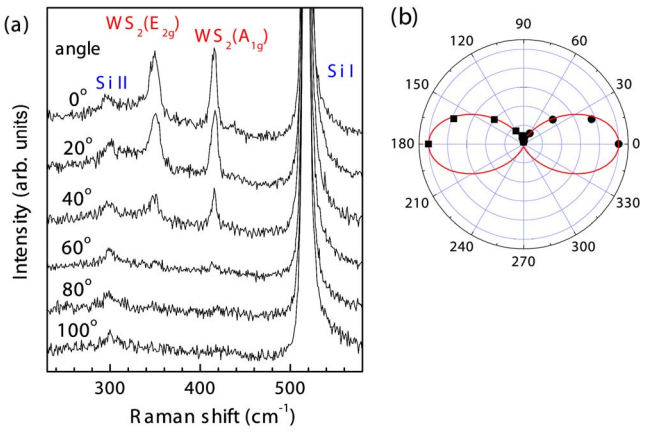

FIG. 3. (Color online) (a) Parallel polarized Raman spectra with different angles of the polarization with respect to the nanotube axis. (b) Angular dependence of the Raman intensity of two WS_2 nanotube modes. The two sets of points are plotted in separate intervals for clarity: for the E_{2g} (A_{1g}) derived mode from 0° to 90°, circles (180° to 90°, squares). The solid line (red) is a fit of Eq. (2) to the data points.

order of magnitude larger. From the pressure coefficient of the E_{2g}-derived mode with a vibrational pattern along both the circumference and the nanotube axis, we determine the two-dimensional (in-plane) Grüneisen parameter and arrive at a value of 0.45. Note the huge difference to the corresponding value of graphite (2.0)[23] emphasizing the softness of the WS_2 nanotube material.

We now give a quantitative estimate of the antenna effect by varying the angle of (parallel) polarization with respect to the nanotube axis, see Fig. 3, where we note the decreasing scattering intensity in going from 0° to 90°. The angular dependence of the Raman intensities, normalized to the spectra at 0°, is shown in a polar plot in Fig. 3. Indeed, we observe a strong antenna effect in WS_2 nanotubes in contrast to MWNTs, where only a weak screening for perpendicular polarized light was found.[13,14] We attribute the strong effect in WS_2 to the large in-plane components of both the real and imaginary part of the dielectric tensor of a 2H-WS_2 layer compared to the out-of-plane components at 1.96 eV.[24] For a nanotube, this translates into a larger dipole moment along the axis than perpendicular to it, even in the absence of an antenna effect. The superimposed screening of the polarizabilities by the antenna effect leads to the observed strong polar behavior of the Raman intensities.

In order to quantify the degree of screening, we modeled the angular dependence of the Raman intensity in Fig. 3 with a polarizability tensor with $\alpha_{XX}=\alpha_{YY}=\varepsilon$; $\alpha_{ij}=0$ for $i\neq j$ and $\alpha_{ZZ}=1$. The unit polarization vectors $e_{i,s}$ of the incident and scattered light were parametrized by their angle φ to the nanotube axis. The relative Raman intensity $I_R=|\langle e_s\cdot\hat{R}\cdot e_i\rangle|^2$ can be written as

$$I_R(\varphi)=(\varepsilon\sin^2\varphi+\cos^2\varphi)^2. \tag{2}$$

We obtained ε through a least square fit of Eq. (2) to the data points in Fig. 3(b): $\varepsilon=\alpha_{XX}=0.175$ for the mode at 417 cm^{-1} and $\varepsilon=0.152$ for the one at 351 cm^{-1}. Taking the average of both, we estimate $\varepsilon=0.16\pm0.05$. We have thus derived the relative components of the polarizability tensor; in the present approximation, it differs from the Raman tensor only by a numeric factor. The theoretical angular dependence of Eq. (2) is also plotted in Fig. 3(b); it gives an excellent quantitative description of the data. Small deviations due to slight bending or buckling of the nanotube may still be present. Therefore, we consider the estimated value of $\varepsilon=0.16$ an upper bound for α_{XX}. This value compares well with $\varepsilon\approx0.09$ obtained from similar experiments[7,8] on SWNTs, given the higher aspect ratio of SWNTs. The strong optical response and its well pronounced angular dependence in WS_2 nanotubes is also an indication of their high structural quality. In fact, a recent study on their mechanical properties showed that WS_2 nanotubes are almost defect free.[21]

The antenna effect in cylindrical nano-objects was studied in the electrostatic limit by Benedict *et al.*, who showed that the screened polarizability per unit length in radial direction is[2,9]

$$\alpha_{XX}(\omega)=\frac{\alpha_{0,XX}(\omega)}{1+2\alpha_{0,XX}(\omega)/R^2}, \tag{3}$$

where R is the cylinder radius and $\alpha_{0,XX}$ is the unscreened polarizability. Considering that, to a crudest approximation, the polarizability of a molecule (in cgs units) corresponds to its volume,[25] we argue that $\alpha_{0,XX}(\omega)$ roughly corresponds to the nanotube's cross section πR^2. This is confirmed by a more sophisticated model for SWNTs where Benedict *et al.*[2] find $\alpha_{0,XX}(\omega)\approx2.6R^2$. Substituting πR^2 for $\alpha_{0,XX}(\omega)$ in Eq. (3) yields a screening factor of the perpendicular polarizability of about 7. The axial component $\alpha_{0,ZZ}=\alpha_{ZZ}$ is not affected by screening provided the nanotube is not capped,[2] which is the typically the case with WS_2 nanotubes.[26] From the dielectric tensor values[24] of bulk WS_2, we estimate $2\leqslant\alpha_{0,ZZ}(\omega)/\alpha_{0,XX}(\omega)\leqslant3$ for $\hbar\omega=1.96$ eV, which finally yields $\alpha_{XX}(\omega)/\alpha_{ZZ}(\omega)\approx0.06$ in reasonable agreement with our experimental results considering the coarseness of the estimate of the static polarizability.

It is particularly puzzling why, in MWNT, an extremely weak depolarization effect was found.[13,14] The use of an agglomerated sample including different nanotube orientations as well as the graphite-like density of states in MWNTs, where van-Hove singularities are largely smeared out, may be explanations for this result. However, the geometric considerations and the anisotropy in the bulk in-plane and out-of-plane dielectric tensor components apply likewise for graphite[27] and should lead to a considerable antenna effect in individual MWNTs. Given the antenna-effect-like reflectivity response of MWNT random arrays reported recently,[15] angular-dependent absorption and polarized Raman experiments on reliably oriented MWNTs are definitely called for.

IV. CONCLUSIONS

In summary, we obtained a Raman spectrum from an individual WS_2 multiwalled nanotube attached to the tip of an AFM cantilever in a well-defined orientation. We confirm the feasibility of simultaneous Raman and mechanical measure-

ments on an individual WS_2 nanotube based on a correlation of the phonon frequency shifts with the elastic response. This can yield deeper insight into the subtle interplay of the nanotubes vibrational and mechanical properties and provide valuable knowledge for various potential applications of WS_2 nanotubes. Combining results from Raman scattering and buckling experiments, we determine the in-plane Grüneisen parameter $\gamma^{2D}=0.45$.

By means of angular-dependent polarization measurements, we established a strong antenna effect in WS_2 multiwalled nanotubes and estimated an upper bound of the ratio $\alpha_{XX}/\alpha_{ZZ}=0.16$ for the perpendicular to parallel polarizability tensor components. We conclude that the antenna effect in cylindrically shaped nano-objects is not restricted to small radii ($\approx$1 nm) or to single-walled carbon nanotubes, but exists for significantly larger radii (20 to 50 nm) as well if the aspect ratio is sufficiently high and if the original layered material has a strongly anisotropic polarizability. Applications exploiting the antenna effect are not restricted to carbon technology, but may use WS_2 or other nanotubes made of layered material as well.

This work was supported by The Minerva Foundation (Munich); The G.M.J. Schmidt Minerva Center for Supramolecular Architectures, the German-Israeli Foundation (GIF), and the NATO Science Foundation.

*Permanent address: Institute of Solid State Physics, Bulgarian Academy of Sciences, Blvd. Tzarigradsko Chausse 72, 1784 Sofia, Bulgaria.

[1] A. Rothschild, S. R. Cohen, and R. Tenne, Appl. Phys. Lett. **75**, 4025 (1999).
[2] L. X. Benedict, S. G. Louie, and M. L. Cohen, Phys. Rev. B **52**, 8541 (1995).
[3] H. Ajiki and T. Ando, Jpn. J. Appl. Phys., Suppl. **34**, 107 (1995).
[4] Z. M. Li, Z. K. Tang, H. J. Liu, N. Wang, C. T. Chan, R. Saito, S. Okada, G. D. Li, J. S. Chen, N. Nagasawa, and S. Tsuda, Phys. Rev. Lett. **87**, 127401 (2001).
[5] K. Kneipp, A. Jorio, H. Kneipp, S. D. M. Brown, K. Shafer, J. Motz, R. Saito, G. Dresselhaus, and M. S. Dresselhaus, Phys. Rev. B **63**, 081401(R) (2001).
[6] A. Jorio, A. G. Souza Filho, V. W. Brar, A. K. Swan, M. S. Ünlü, B. B. Goldberg, A. Righi, J. H. Hafner, C. M. Lieber, R. Saito, G. Dresselhaus, and M. S. Dresselhaus, Phys. Rev. B **65**, 121402(R) (2002).
[7] G. S. Duesberg, I. Loa, M. Burghard, K. Syassen, and S. Roth, Phys. Rev. Lett. **85**, 5436 (2000).
[8] P. M. Rafailov, J. Maultzsch, M. Machon, S. Reich, C. Thomsen, Z. K. Tang, Z. M. Li, and I. L. Li, in *Molecular Nanostructures*, edited by H. Kuzmany, M. Mehring, S. Roth, and J. Fink (AIP, Melville, NY, 2002), p. 290.
[9] S. Reich, C. Thomsen, and J. Maultzsch, *Carbon Nanotubes: Basic Concepts and Physical Properties* (Wiley-VCH, Weinheim, 2004).
[10] H. H. Gommans, J. W. Alldredge, H. Tashiro, J. Park, J. Magnuson, and A. G. Rinzler, J. Appl. Phys. **88**, 2509 (2000).
[11] R. Krupke, F. Hennrich, H. von Löhneysen, and M. M. Kappes, Science **301**, 344 (2003).
[12] A. G. Marinopoulos, L. Reining, A. Rubio, and N. Vast, Phys. Rev. Lett. **91**, 046402 (2003).
[13] A. M. Rao, A. Jorio, M. A. Pimenta, M. S. S. Dantas, R. Saito, G. Dresselhous, and M. S. Dresselhous, Phys. Rev. Lett. **84**, 1820 (2000); S. Reich and C. Thomsen, Phys. Rev. Lett. **85**, 3544 (2000).
[14] X. Zhao, Y. Ando, Y. Liu, M. Jinno, and T. Suzuki, Phys. Rev. Lett. **90**, 187401 (2003).
[15] Y. Wang, K. Kempa, B. Kimball, J. B. Carlson, G. G. Benham, W. Z. Li, T. Kempa, J. Rybczynski, A. Herczynski, and C. F. Ren, Appl. Phys. Lett. **85**, 2607 (2004).
[16] G. Frey, R. Tenne, M. J. Matthews, M. S. Dresselhaus, and G. Dresselhaus, J. Mater. Res. **13**, 2412 (1998).
[17] J. Maultzsch, S. Reich, U. Schlecht, and C. Thomsen, Phys. Rev. Lett. **91**, 087402 (2003).
[18] C. Thomsen, Phys. Rev. B **61**, 4542 (2000).
[19] M. Cardona, in *Light Scattering in Solids II*, edited by M. Cardona and G. Günterodt (Springer Verlag, Berlin, 1982).
[20] I. Kaplan-Ashiri, S. R. Cohen, K. Gartsman, F. Rosentsveig, G. Seifert, and R. Tenne, J. Mater. Res. **19**, 454 (2004).
[21] I. Kaplan-Ashiri, S. R. Cohen, K. Gartsman, V. Ivanovskaya, T. Heine, G. Seifert, I. Kanevsky, H. D. Wagner, and R. Tenne (unpublished).
[22] C. Thomsen, S. Reich, H. Jantoljak, I. Loa, K. Syassen, M. Burghard, G. S. Duesberg, and S. Roth, Appl. Phys. A: Mater. Sci. Process. **69**, 309 (1999).
[23] C. Thomsen, S. Reich, and P. Ordejon, Phys. Rev. B **65**, 073403 (2002).
[24] D. Taverna, M. Kociak, V. Charbois, and L. Henrard, Phys. Rev. B **66**, 235419 (2002).
[25] J. D. Jackson, *Classical Electrodynamics*, 2nd ed. (Wiley, New York, 1975).
[26] G. Seifert, T. Köhler, and R. Tenne, J. Phys. Chem. B **106**, 2497 (2002).
[27] O. Stephan, D. Taverna, M. Kociak, K. Suenaga, L. Henrard, and C. Colliex, Phys. Rev. B **66**, 155422 (2002).